Journal of Rajasthan Academy of Physical Sciences
ISSN: 0972-6306; URL: http://raops.org.in
Vol.20, No.3&4, July-December, 2021, 149-164

ENTROPY GENERATION EFFECT IN MHD FLOW THROUGH A POROUS HORIZONTAL CHANNEL IN THE PRESENCE OF SLIP BOUNDARY CONDITIONS AND POROUS MEDIA

Aastha[1], Khem Chand[2] and Jyoti Prakash[3]
[1]Department of Mathematics and Statistics, Himachal Pradesh University, Shimla
E-mail: [1]aastha2101@gmail.com (corresponding author)
[2&3]Department of Mathematics and Statistics, Himachal Pradesh University, Shimla
E-mail: [2]khemthakur99@gmail.com, [3]jpsmaths67@gmail.com

Abstract: In the present paper, combined effect of magnetic field, porous media and slip flow conditions on the entropy generation in the flow of an incompressible and electrically conducting fluid in an infinite horizontal porous channel under a constant pressure gradient have been carried out. The dimensional ordinary differential equations of motion and energy are transformed to non-dimensional form by using the relevant non-dimensional variables. The exact solutions of governing equations and its numerical calculations have been done by using Matlab function 'bvp4c'. The effect of different governing parameters on velocity, temperature, entropy generation are elaborated with the help of tables and graphs. It is concluded from this study that for increase in the magnetic parameter, slip parameters, group parameter, Brinkmann number, Peclet number and Darcy number, the entropy generation N_s increase near the lower plate whereas the entropy generation decreases with the increase in the Reynold's number.

Keywords: Entropy generation number; Bejan number; Brinkmann number; Peclet number; Reynold's number; Magnetic parameter.

Mathematics Subject Classification: 76D05, 65P99

1. Introduction

The second law of thermodynamics analysis is the basis in the area of heat transfer along with thermal design and the structure given by it correlates the hypothesis of entropy generation minimization. The Clasius and Kelvin studied the aspects of irreversibility of the Second law of Thermodynamics and initiated the knowledge of entropy production [1,8,10]. Bejan [2,7] noticed the sources of entropy generation in the process of conventional heat transfer problem. The author entrenched that during the process of flowing of fluid, the production of entropy was ascribed to the finite differences in velocity gradient and the temperature. In fluid dynamics, due to abnormal accord with the results in

the experiment for a century, the studies fail to mention that no slip condition remains a supposition. However, another approach assumed that fluid can slide over a solid surface. Navier [24] presented the slip of fluid at the solid boundary with the help of general boundary conditions. He gave the proposal that at the solid surface, the velocity is proportional to the shear stress. The concept of slip occurrence has been exhibited by many theoretical and experimental studies like Gbadeyan et al. [14], Mahmoud and Waheed [18], Martin and Boyd [21], Mehmood [22]. They examined that rise in the slip parameter slows down the process of flow of fluid. In a channel with permeable boundaries, the effect of slip conditions on hydromagnetic steady flow in a channel with permeable boundaries were given by Khalid and Wafai [17] and Makinde and Osalusi [19] obtained the solution in closed form for steady periodic and transient velocity field with slip conditions. To look into the irreversibilities in terms of the rate of entropy generation, the second law of thermodynamics is applicable. Bejan [9] worked into the second law of thermodynamics by virtue of entropy generation minimization specifically in the area of thermal science, heat transfer, storage and thermal power conversion. The entropy generation minimization studies has procured significant attention in many energy involving problems including thermal energy, cooling of the modern electronic system, geothermal energy system and solar power collectors. In any thermal process, the study of entropy generation gives a useful technique for determining the irreversibility in any thermal process.

The irreversibility occurrence for a microfluidic flow is due to heat and mass transfer, friction dissipation or chemical reaction. Makinde [20] discussed the Entropy analysis for MHD boundary layer flow and heat transfer over a flat plate with a convective surface boundary condition. Akbar [5] investigated the entropy generation and energy conversion rate for the peristaltic flow in a tube with magnetic field. Different aspects of magnetohydrodynamic flow and thermal conductance phenomena have been carried out by various researchers, for details see [4,6]. Jian [16] studied the MHD flow and entropy generation in microchannel with electroosmotic effects. The analysis of the effects of mixed convection and entropy generation on an MHD nanofluid flow is done by Fersadou et al. [13]. Ibanez et al. [15] assessed the impact of magnetic field and entropy generation on nanofluid flow towards a micro-channel. Nasiri et al. [23] investigated the consequences of the magnetic field on entropy generation towards a microchannel. Shi and Dong [26] have reviewed the entropy generation and heat transfer flow through a microchannel.

The primary objective of the present analysis is to examine the combined effects of magnetic field, suction / injection and Navier slips on entropy generation in a MHD flow through a porous channel under a constant pressure gradient. The solutions in closed form have been obtained for the velocity and temperature of the fluid. The various plots have been displayed which have been obtained with the help of Matlab function ‘bvp4c’ of the solution of given boundary value problem. The effect of different parameters involving in the governing equations of the problem on velocity flow, temperature flow, entropy generation and Bejan number have been studied.

2. Mathematical Formulation of the problem

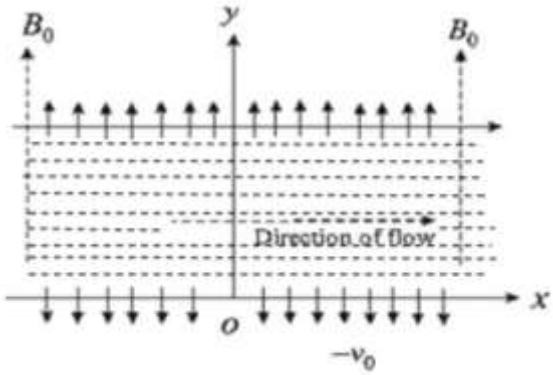

Fig A. Geometrical configuration of the problem

Let us have a viscous incompressible electrically conducting fluid enclosed between two infinite horizontal parallel porous plates at a distance 'h' apart. Let us have x-axis along the lower stationery plate which is also the direction of flow of fluid and y-axis perpendicular to the plates in the cartesian coordinate system. The uniform transverse magnetic field B_0 is in the direction perpendicular to the plates of the channel. Due to the infinite length of the plates, all physical variables excluding pressure are dependant only upon y.

The basic fundamental equations of fluid dynamics then become:

Equation of Continuity:

$v = -v_0$ where $v_0$is the suction velocity at the plates

Equation of Motion:

$$-v_0 \frac{du}{dy} = -\frac{1}{\rho}\frac{\partial \rho}{\partial x} + \upsilon \frac{d^2u}{dy^2} - \sigma \frac{B_0^2}{\rho} u - \frac{\upsilon u}{k} \tag{1}$$

Equation of Energy:

$$-v_0 \frac{dT}{dy} = \frac{k}{\rho C_p}\frac{d^2T}{dy^2} + \frac{\mu}{\rho C_p}\left(\frac{du}{dy}\right)^2 + \lambda \frac{\sigma B_0^2}{\rho C_p} u^2 \tag{2}$$

where μ is the fluid velocity at x-axis, ρ is the fluid density, ν the kinematic viscosity, σ the electrical conductivity of the fluid and p is the fluid pressure, μ is the coefficient of viscosity, k the thermal conductivity, C_p the specific heat at constant pressure, the index λ in the equation (2) is taken equal to 1 for including Joule dissipation.

The relevant boundary conditions are as follows:

$$\mu = \gamma_1 \frac{du}{dy}, T = T_0 \; at \; y = 0$$

$$\mu = \gamma_2 \frac{du}{dy}, T = T_h \; at \; y = h \tag{3}$$

where T is the temperature of the fluid, T_h is the upper plate temperature,T_0 is the lower plate temperature and γ_1 and $\gamma_2$are the slip coefficients.

Non-dimensionalising the equations, we introduce the non-dimensional variables as-

$$\eta = \frac{y}{h}, w_1 = \frac{u}{v_0}, \varphi = \frac{T-T_0}{T_h-T_0} \tag{4}$$

From Eqs. (1) and (2), we then have

$$\frac{d^2w_1}{d\eta^2} + Re\frac{dw_1}{d\eta} - \left(M^2 + \frac{1}{D_a}\right)w_1 = -P \tag{5}$$

$$\frac{d^2\varphi}{d\eta^2} + Pe\frac{d\varphi}{d\eta} + Br\left[\left(\frac{dw_1}{d\eta}\right)^2 + \lambda M^2 w_1^2\right] = 0 \tag{6}$$

here $M^2 = \frac{\sigma B^2 h^2}{\rho v}$ is the magnetic parameter, $Br = \frac{\mu v_0^2}{k(T_h - T_0)}$ the Brinkmann number, $Pe = \frac{v_0 h \rho C_p}{k}$ the Peclet number, $Re = \frac{v_o\ h}{\nu}$ the Reynold's number, $D_a = \frac{k}{h^2}$ is the Darcy number and $P = \frac{h^2}{\rho v v_0}\left(-\frac{\partial p}{\partial x}\right)$ is the non-dimensional pressure gradient.

The boundary conditions for the above problem is:

$$w_1 = \alpha_1 \frac{dw_1}{d\eta}, \varphi = 0\ at\ \eta = 0$$

$$w_1 = \alpha_2 \frac{dw_1}{d\eta}, \varphi = 1\ at\ \eta = 1 \tag{7}$$

where $\alpha_1 = \frac{\gamma_1}{h}$ and $\alpha_2 = \frac{\gamma_2}{h}$ are the slip parameters.

The solutions of the equations subject to these boundary conditions are given by -

$$w_1(\eta) = \frac{P}{(M^2 + \frac{1}{D_a})} + (A\cosh n\eta + B\sinh n\eta)e^{\frac{-Re}{2}\eta} \tag{8}$$

where $n = \frac{[Re^2 + 4(M^2 + \frac{1}{D_a})]^{1/2}}{2}$

The solution given by the Eq. (8) is applied for both Re< 0 (for the blowing at the plates $v_0 < 0$) and $Re > 0$ (for the suction at the plates $v_0 > 0$).

By solving equation (8), equation (6) becomes

$$\frac{d^2\varphi}{d\eta^2} + Pe\ \frac{d\varphi}{d\eta} = -Br[e^{-Re\eta}\{A_1 + \frac{1}{2}(A_4\cosh 2n\eta + A_5\sinh 2n\eta)\} + \frac{2\lambda P}{\left(1+\frac{1}{D_a M^2}\right)}e^{\frac{-Re}{2}\eta}(A\cosh n\eta + B\sinh n\eta) + \frac{\lambda P^2}{(1+\frac{1}{D_a M^2})^2}] \tag{9}$$

Solution of the equation (11) subject to the boundary conditions is -

$$\varphi(\eta) = c_1 + c_2 e^{-Pe\eta} - Br\left[e^{-Re\eta}\left\{A_8 + \frac{1}{2}(A_4\cosh 2n\eta + A_5\sinh 2n\eta) + \frac{\lambda P e^{\frac{-Re}{2}\eta}}{(1+\frac{1}{D_a M^2})}(A_6\cosh n\eta + A_7\sinh n\eta) - \frac{\lambda P^2}{Pe(1+\frac{1}{D_a M^2})}\eta\right\}\right] \tag{10}$$

3. Discussion of the results

The rate of heat transfer at the plates $\eta = 0$ and $\eta = 1$ are procured as -

$$\varphi'(0) = -c_2 \mathrm{Pe} + \mathrm{Br}\left[\left\{\mathrm{ReA}_8 + \left(\mathrm{Re}\frac{\mathrm{A}_4}{2} + 2\mathrm{n}\frac{\mathrm{A}_5}{2}\right)\right\} + \frac{\lambda \mathrm{P}}{\left(1+\frac{1}{\mathrm{D_a M^2}}\right)}\left(\mathrm{nA}_7 - \frac{\mathrm{Re}}{2}\mathrm{A}_6\right) + \frac{\lambda \mathrm{P}^2}{\mathrm{Pe}\left(1+\frac{1}{\mathrm{D_a M^2}}\right)^2}\right] \quad (11)$$

$$\varphi'(1) = -c_2 Pe\, e^{-Pe} + Br\left[e^{-Re}\left\{ReA_8 + \left(Re\frac{A_4}{2} + 2n\frac{A_5}{2}\right)\cosh 2n + \left(Re\frac{A_5}{2} + 2n\frac{A_4}{2}\right)\sinh 2n\right\} - \frac{\lambda Pe^{\frac{-Re}{2}}}{\left(1+\frac{1}{D_a M^2}\right)}\left\{\left(\frac{1}{2}ReA_6 + nA_7\right)\cosh n + \left(\frac{1}{2}ReA_7 + nA_6\right)\sinh n\right\} + \frac{\lambda P^2}{Pe\,(1+\frac{1}{D_a M^2})}\right] \quad (12)$$

All the constants used above have been given in the appendix.

Table 1 :-Rate of heat transfer at the plates $\eta = 0$ and $\eta = 1$ when $Br = 2, \alpha_1 = 0.1, \alpha_2 = 0.1, Pe = 3$ and $D_a = 0.2$

R/M^2	$\varphi'(0)$				$\varphi'(1)$			
	5	10	15	20	5	10	15	20
0.5	3.3462	3.2283	3.2166	5.2289	-0.1115	-0.0168	-0.0992	-12.5320
1.0	3.3376	3.2232	3.2072	5.0843	-0.0752	-0.0074	-0.0475	-11.6497
1.5	3.3297	3.2190	3.2002	3.6512	-0.0446	0.0272	-0.0098	-2.7874
2.0	3.3222	3.2154	3.1949	3.3828	-0.0188	0.0435	0.0185	-1.1486

Table 2 :-Rate of heat transfer at the plates $\eta = 0$ and $\eta = 1$ when $Re = 2, \alpha_1 = 0.1, \alpha_2 = 0.1, M^2 = 5$ and $D_a = 0.2$

Br/Pe	$\varphi'(0)$				$\varphi'(1)$			
	4	6	8	10	4	6	8	10
0.2	4.1354	6.1657	8.2875	10.4639	0.0428	-0.0426	-0.0829	-0.1149
0.4	4.1962	6.3166	8.5724	10.9274	0.0110	-0.1001	-0.1685	-0.2302
0.6	4.2570	6.4674	8.8572	11.3908	-0.0209	-0.1577	-0.2540	-0.3455
0.8	4.3177	776.6182	9.1421	11.8543	-0.0527	-0.2152	-0.3396	-0.4608

Table 3:-Rate of Heat transfer at the plates $\eta = 0$ and $\eta = 1$ when $Re = 2, Pe = 3, Br = 1, M^2 = 5$ and $D_a = 0.2$

α_1/α_2	$\varphi'(0)$				$\varphi'(1)$			
	0.2	**0.5**	**0.8**	**1.1**	**0.2**	**0.5**	**0.8**	**1.1**
0.3	3.3453	5.2264	3.6816	3.5594	-0.0810	-2.2341	-0.2162	-0.0814
0.5	3.3523	5.2354	3.6852	3.5632	-0.0835	-2.2588	-0.2194	-0.0836
0.7	3.3576	5.2462	3.6903	3.5682	-0.0850	-2.2730	-0.2214	-0.0850
0.9	3.3616	5.2533	3.6949	3.5725	-0.0860	-2.2823	-0.2227	-0.0859

The rate of heat transfer $\varphi'(0)$ and $\varphi'(1)$ is displayed in Tables 1 to 3 numerically for various values of different parameters such as M^2, Re, Br, Pe, D_a, α_1 and α_2. From Table 1, it is noticed that the rate of heat transfer $\varphi'(0)$ decreases with an increase in Reynold's number Re while for increase in magnetic parameter M^2, it decreases near the surface and it increases away from the surface. Also, it can be seen that the rate of heat transfer $\varphi'(1)$ at the plate $\eta = 1$ increases as the Reynold's number Re increases and decreases as the magnetic parameter M^2 decreases. From Table 2, we find that the rate of heat transfer increases for increase in the both Brinkmann number (Br) and the Peclet number(Pe) at the plates η=0. On the other hand, at the plates η=1, the rate of heat transfer decreases for the increase in Brinkmann number(Br) as well as the Peclet number Pe. From Table 3, it is expressed that the rate of heat transfer at the plate η=0 increases with an increase in slip parameter α_1 whereas for the slip parameter α_2, the rate of heat transfer increases near the plate and decreases away from the plate. The rate of heat transfer $\varphi'(1)$ at the plate η=1 shows a decrease with the increase in the slip parameter α_1 and for the increase in the slip parameter α_2, it decreases near the plate and increases away from the plate.

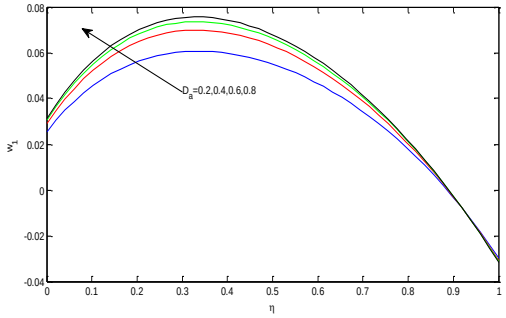

Figure 1 Velocity profiles for different D_a when $M^2 = 5$, $\alpha_1 = 0.1$,$\alpha_2 = 0.1$, $Re = 2$ and $D_a = 0.2$

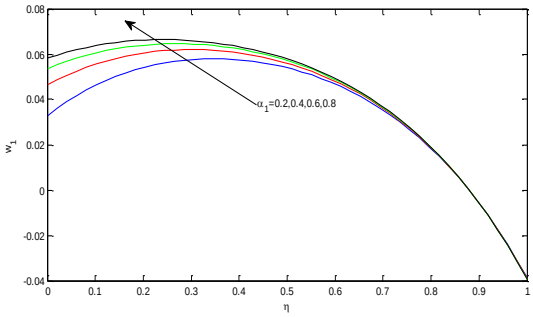

Figure 2 Velocity profiles for different α_1 when $M^2 = 5$, $\alpha_2 = 0.1$, $Re = 0.5$ and $D_a = 0.2$

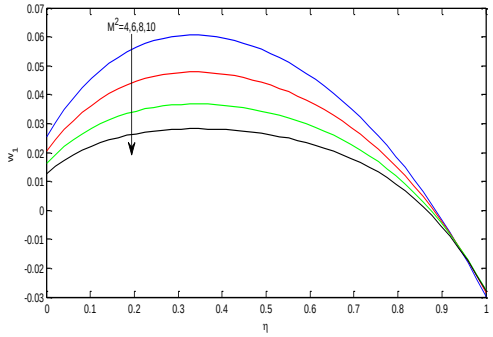

Figure 3 Velocity profiles for different M^2 when $Re = 2, \alpha_1 = 0.1$,$\alpha_2 = 0.1$ and $D_a = 0.2$

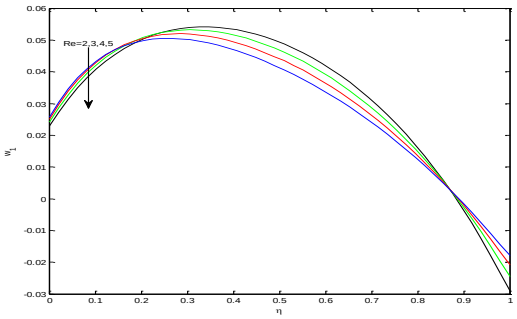

Figure 4 Velocity profiles for different Re when $M^2 = 5$, $\alpha_1 = 0.1$,$\alpha_2 = 0.1$ and $D_a = 0.2$

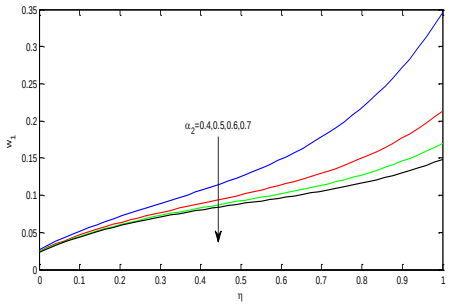

Figure 5 Velocity profiles for different α_2 when $M^2 = 5$, $\alpha_1 = 0.1, Re = 0.1$ and $D_a = 0.2$

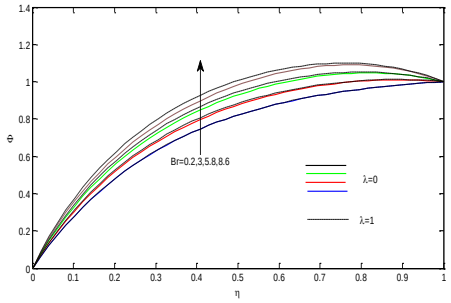

Figure 6 Temperature profiles for different Br when $Re = 2, D_a = 0.2$ and $Pe = 3$

The non-dimensional velocity w_1 has been plotted against η the space coordinate for studying the effects of magnetic field and Reynold's number on the velocity. It is seen from figures (1 to 5) that the velocity of the fluid shows an increase with the increase in the Darcy number (D_a) and slip parameter(α_1) while for the magnetic parameter (M^2), Reynold's number(Re) and slip parameter (α_2), it diminishes. The Lorentz force causes the resistance to the flow of the fluid resulting in the decrease in the fluid velocity. The larger is the value of the Reynold's number, the higher is the strength of suction/injection showing a decrease in the velocity of the fluid as represented in Figure 2.

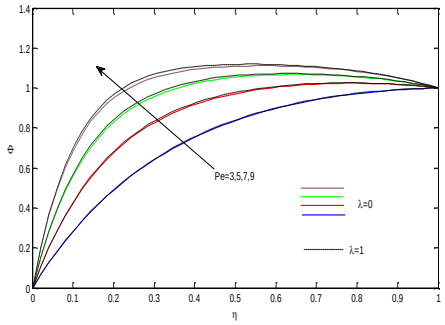

Figure 7 Temperature profiles for different Pe when $Br = 1, D_a = 0.2$ and $Re = 2$

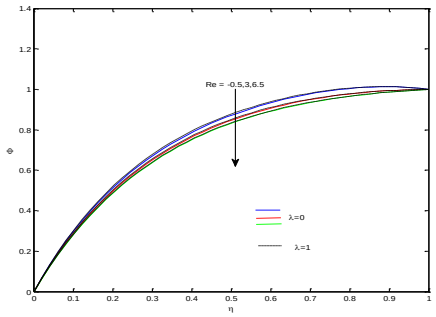

Figure 8 Temperature profiles for different Re when $Br = 1, Pe = 3$ and $D_a = 0.2$

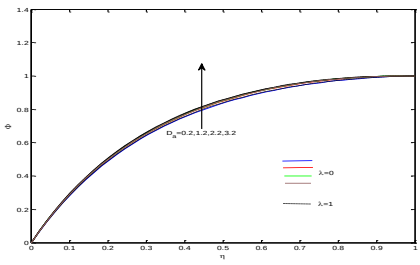

Figure 9 Temperature profiles for different D_a when $Br = 1, Pe = 3$ and $Re = 2$

In case of the temperature profiles, the temperature of the fluid has been displayed in the figures(6 to 9). From the graphs, it is evident that the temperature of the fluid increases with the increase in the Brinkmann number(Br) and Peclet number(Pe) whereas the temperature decreases with the decrease in the Reynold's number (Re). Darcy number(D_a) don't have any significant effect on the temperature field as illustrated in Figure 9.

5. Entropy Generation

Physically, entropy is the disorder of a system and the surrounding.In microscopic level, it occurs when heat transfer occurs because heat is a energy, when it moves some additional movement happens eg molecular friction, molecular vibration, internal displacement of molecule, spin moment, kinetic energy etc. which make loses useful heat, thus heat can't be transformed fully into work. This additional movements create chaos in the system and the surroundings, that's why sometimes entropy is called the measure of the chaos. For this, microscopic chaos results in macroscopic level which occurs because some unnecessary irreversibilities eg friction, mixing of fluids, electric resistance, inelastic deformation of solids, chemical reaction and unnecessary heat transfer in finite temperature difference. Noting that such kind of energy loss can't be regained so system and surrounding can't come to its initial state without extra work done on it. Therefore, Entropy is called the measure of irreversibilities.For this cause, heat can't be transformed fully into work. In real life, all sort of process has this kind of macroscopic and microscopic loss. So in reality each and every thermodynmanic process is an irreversible process. So in reality each and every thermodynamic process is an irreversible process.

Entropy generation occurs due to irreversiblity of process or in simple terms due to irreversibility of process or in simple terms due to friction associated during the process. Entropy generation is zero for reversible process. Woods[27] has indicated the local volumetric rate of entropy generation for a viscous incompressible conducting fluid in the presence of magnetic field as:

$$E_G = \frac{k}{{T_0}^2}\left(\frac{dT}{dy}\right)^2 + \frac{\mu}{T_0}\left(\frac{du}{dy}\right)^2 + \lambda\frac{\sigma B_0^2}{T_0}u^2 \tag{13}$$

The entropy generation above comprises of three terms, the first one is the irreversibility due to the heat transfer, the second one is the entropy generation due to viscous dissipation and the last one is local entropy generation due to the effect of magnetic field. (Joule heating or Ohmic heating)

The entropy generation number in dimensionless form is given as:

$$N_s = \frac{T_0^2 h^2 E_G}{k(T_h - T_{0)}} \tag{14}$$

For velocity and temperature without dimensions, the entropy generation number is given as:

$$N_s = \left(\frac{d\varphi}{dy}\right)^2 + \frac{Br}{\Omega}\left[\left(\frac{dw_1}{d\eta}\right)^2 + \lambda M^2 w_1^2\right]$$

where $Br = \frac{\mu v_0^2}{k(T_h - T_0)}$ is the Brinkmann number and $\Omega = \frac{T_h - T_0}{T_o}$, the non dimensional temperature difference.

The entropy generation number is written as a combination of the entropy generation due to heat transfer given by N_1 and the entropy generation due to fluid friction with magnetic field denoted by N_2 given as,

$$N_1 = \left(\frac{d\varphi}{d\eta}\right)^2, N_2 = \frac{Br}{\Omega}\left[\left(\frac{dw_1}{d\eta}\right)^2 + \lambda M^2 w_1^2\right]$$

Paoletti et al[25] introduced an alternative irreversibility distribution parameter in terms of Bejan number(Be) which is given as:

Be $= \frac{N_1}{N_s} = \frac{1}{1+\epsilon}$

where $\epsilon = \frac{N_2}{N_1}$ is the irreversibility ratio.

When $0 \leq \epsilon < 1$, heat transfer is prepotent while for $\epsilon > 1$, fluid friction with magnetic effects is ascendant. Heat transfer and fluid friction both have influence of same magnitude to entropy generation for $\epsilon = 1$. From [12], it is clear that the Bejan number (Be) has its values lying between 0 and 1. It approaches zero when the entropy generation due to the combined effects of fluid friction and magnetic field is dominant. Similarly, Be = 0.5 indicates that the irreversibility due to heat transfer dominates with Be=1 as the limit at which the irreversibility is solely due to heat transfer.

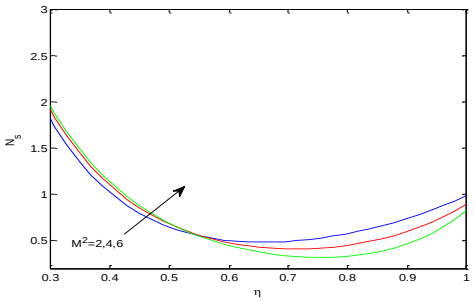

Figure10 N_s for different $M^2$when $Pe = 3, \alpha_1 = 0.1, \alpha_2 = 0.1, Br = 1, Br\Omega^{-1} = 1, Re = 2$ and $D_a = 0.4$

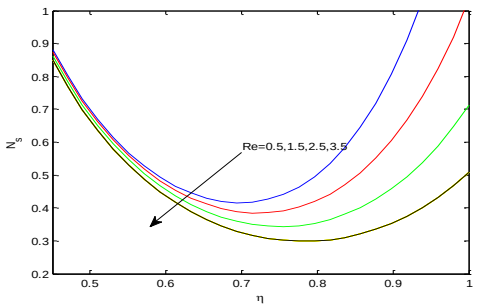

Figure11 N_s for different Re when $Pe = 2, \alpha_1 = 0.1, \alpha_2 = 0.1, Br = 1, Br\Omega^{-1} = 1, M^2 = 5$ and $D_a = 0$.

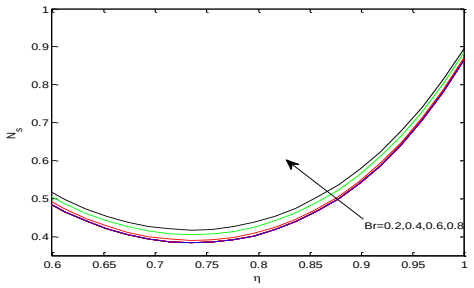

Figure12 N_s for different Br when $Pe = 2, \alpha_1 = 0.1, \alpha_2 = 0.1, Re = 2, Br\Omega^{-1} = 1, M^2 = 5$ and $D_a = 0$

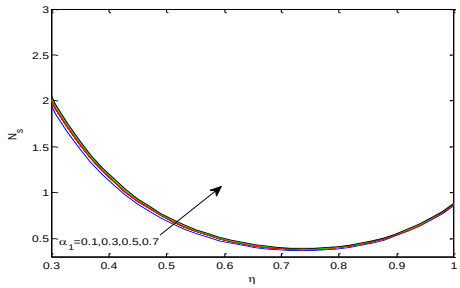

Figure13 N_s for different α_1 when $Pe = 3, Re = 2, \alpha_2 = 0.1, Br = 1, Br\Omega^{-1} = 1, M^2 = 5$ and $D_a = 0.4$

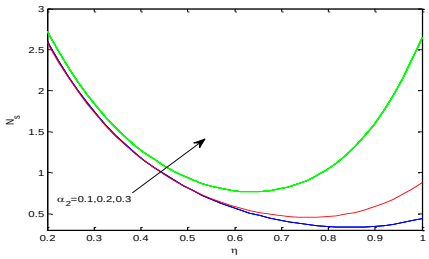

Figure 14 N_s for different α_2 when $Pe = 3, Re = 2, \alpha_1 = 0.1, Br = 1, Br\Omega^{-1} = 1, M^2 = 5$ and $D_a = 0.4$

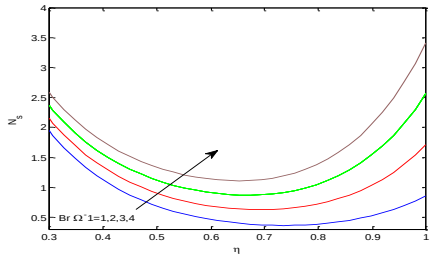

Figure 15 N_s for different $Br\Omega^{-1}$ when $Pe = 3, Re = 2, \alpha_1 = 0.1, \alpha_2 = 0.1, Br = 1, M^2 = 5$ and $D_a = 0.4$

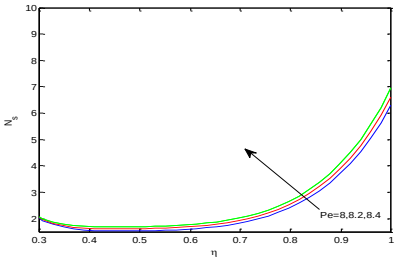

Figure 16 N_s for different Pe when $Re = 2, \alpha_1 = 0.1, \alpha_2 = 0.1, Br = 1, Br\Omega^{-1} = 1, M^2 = 5$ and $D_a = 0.4$

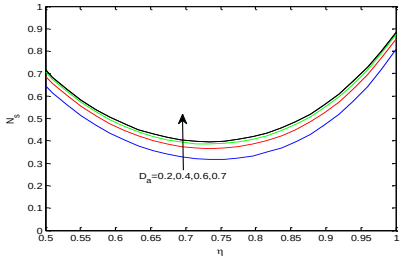

Figure 17 N_s for different D_a when $Re = 2, \alpha_1 = 0.1, \alpha_2 = 0.1, Pe = 3, Br = 1, Br\Omega^{-1} = 1$ and $M^2 = 5$

The impact of various controlling parameters on the entropy generation is given in the figures (10 to 17). Figure 10 shows that the entropy generation N_s increases near the lower plate of the channel and far away from it the reverse trend is exhibited. Figure 11 shows that the increase in the Reynold's number leads to the decrease in the entropy generation rate. From figure (12 to 17), it is found that the entropy generation number increases with the increase in Brinkmann number(Br), slip parameter (α_1) and (α_2), group parameter $(Br\Omega^{-1})$, Peclet number(Pe) and Darcy number(D_a).The temperature gradient within the channel has an increase in its value due to increase in the temperature of the fluid, as a result the entropy generation number has a rise in its value. The enhancement in the values of entropy generation number with an increase in group parameter $Br\Omega^{-1}$ is observed due to increase in the irreversibility of the fluid friction.

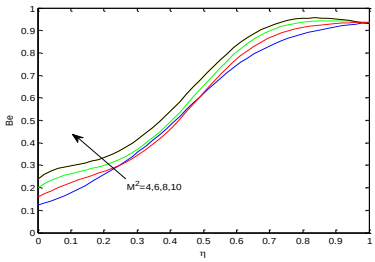

Figure18 Bejan number for different M^2 when $Re = 2, \alpha_1 = 0.1, \alpha_2 = 0.1, Br = 1, Br\Omega^{-1} = 1, D_a = 0.4$ and $Pe = 3$

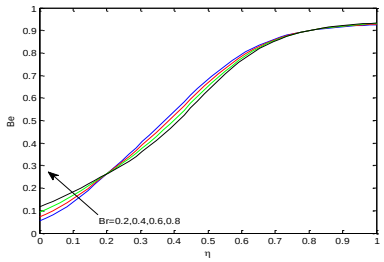

Figure 19 Bejan number for different Br when $M^2 = 5, Re = 2, \alpha_1 = 0.1, \alpha_2 = 0.1, Br\Omega^{-1} = 1, D_a = 0.4$ and $Pe = 3$

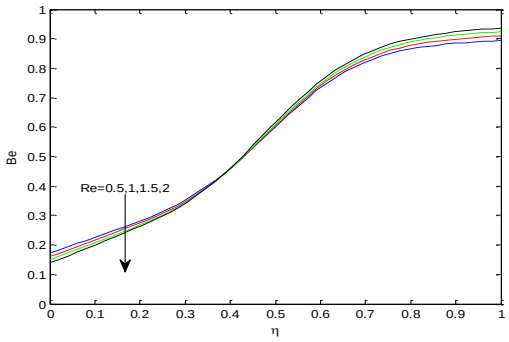

Figure 20 Bejan number for different Re when $M^2 = 5$, $Br = 1$,$\alpha_1 = 0.1, \alpha_2 = 0.1, Br\Omega^{-1} = 1, D_a = 0.4$ and $Pe = 3$

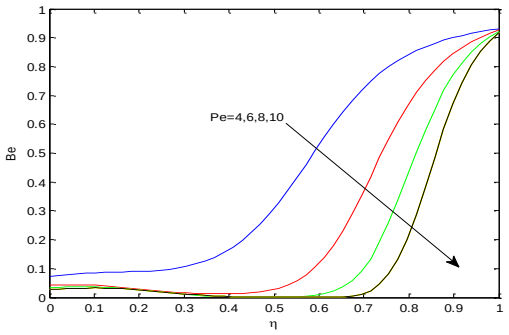

Figure 21 Bejan number for different Pe when $M^2 = 5$, $Br = 1$,$\alpha_1 = 0.1, \alpha_2 = 0.1, Br\Omega^{-1} = 1, D_a = 0.4$ and $Re = 2$

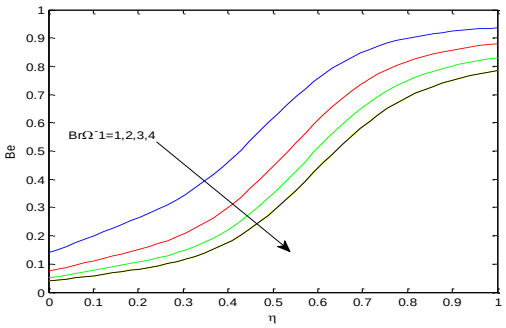

Figure 22 Bejan number for different $Br\Omega^{-1}$ when $M^2 = 5$, $Br = 1$,$\alpha_1 = 0.1, \alpha_2 = 0.1, Pe = 3, D_a = 0.4$ and $Re = 2$

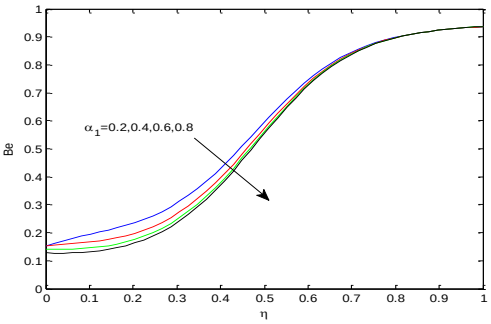

Figure 23 Bejan number for different α_1 when $M^2 = 5$, $Br = 1, \alpha_2 = 0.1, Pe = 3, D_a = 0.4, Br\Omega^{-1} = 1$ and $Re = 2$

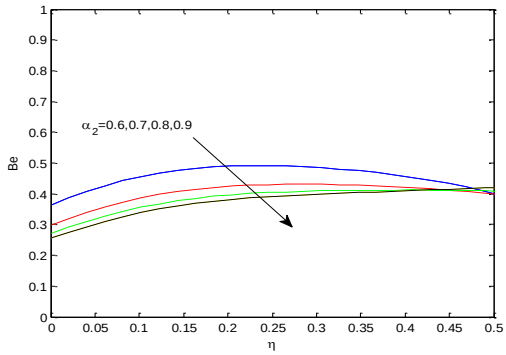

Figure 24 Bejan number for different α_2 when $M^2 = 5$, $Br = 1, \alpha_1 = 0.1, Pe = 3, D_a = 0.4, Br\Omega^{-1} = 1$ and $Re = 2$

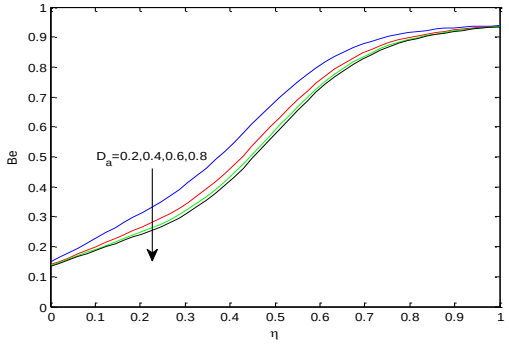

Figure 25 Bejan number for different D_a when $M^2 = 5$, $Br = 1, \alpha_1 = 0.1,\ \alpha_2 = 0.1, Pe = 3, Br\Omega^{-1} = 1$ and $Re = 2$

Now the effect of various parameters on Bejan number(Be) is shown in the figures (17 to 24).It is clear from these figures that the Bejan number(Be) shows an increase with the increasing Magnetic parameter(M^2) and Brinkmann number(Br).On the other hand ,it

reduces with the increasing parameters Reynold's number(Re),Peclet number(Pe),group parameter($\mathrm{Br}\Omega^{-1}$),slip parameter (α_1) and (α_2) and Darcy number(D_a).Group parameter plays an important role in analyzing the irreversibility. The viscous effects to that of temperature gradient entropy generation are governed by this number. It is observed from the figures that the Bejan number(Be) shows a decrease near the lower plate $\eta = 0$ while it increases near the upper plate $\eta = 1$ with the increase in the Reynold's number(Re).

6. Closing Remarks

The combined effect of viscous dissipation, magnetic field, porous media, suction/ injection and slip conditions on entropy generation in a fluid through horizontal porous channels have been investigated. To obtain the entropy production, the analytical results obtained for the velocity and temperature profiles have been used. The velocity and temperature profiles have been plotted by solving equations (5) & (6) with the help of 'bvp4c' function in Matlab software[see(3)]. The non-dimensional entropy generation number and Bejan number have been resolved. The effects of various parameters on the entropy generation number and the rate of heat transfer have been discussed. It is observed that:

1. Velocity of the fluid increases with the increase in the Darcy number and slip parameter α_1 while for magnetic parameter, Reynold's number and slip parameter α_2, it decreases.
2. Temperature of the fluid increases with the increase in the Peclet number and Brinkmann number whereas the temperature decreases with the increase in the Reynold's number. Also, Darcy number don't have much effect on the temperature of the fluid.
3. For increase in the magnetic parameter, the entropy generation N_s increase near the lower plate of the channel and far away from it, it decreases. Alongwith, the entropy generation decreases with the increase in the Reynold's number while it shows an increase with Brinkmann number, slip parameters α_1 and α_2,group parameter, Peclet number and Darcy number.
4. Bejan number shows an increase with the increase in magnetic parameter and Brinkmann number and reduces with the increase in Reynold's number, Peclet number, group parameter, slip parameters α_1 and α_2 and Darcy number.

The entropy generation optimization is helpful to engineer and scientists for designing thermal systems with lesser loss of energy as a result there is availability of maximum possible energy.

Acknowledgement: The authors are thankful to the Referee for valuable comments and suggestions.

References

[1] Bejan, A. (1996), Entropy Generation Minimization, CRC: Boca Raton, NY, USA.

[2] Bejan, A. (1982). Entropy Generation through Heat and Fluid Flow; John Wiley and Sons: New York, NY, USA.

[3] Shampine, L.F., Gladwell, I., Thompson, S. (2003), Solving ODEs with MATLAB, Cambridge University Press, New York.

[4] Aiboud, S., Saouli, S. (2010). Entropy analysis for viscoelastic magnetohydrodynamic flow over a stretching surface, Int. J Non-Linear Mech, **45**, 482-489.

[5] Akbar, N.S. (2015). Entropy generation and energy conversion rate for the peristaltic flow in a tube with magnetic field, Energy, **82**, 23-30.

[6] Akbar, N.S., Raza, M., Ellahi, R. (2015). Peristaltic flow with thermal conductivity of $H_2O + Cu$ nanofluid and entropy generation, Result in Phys, **5**, 115-124.

[7] Bejan, A. (1979). A study of entropy generation in fundamental convective heat transfer, J. Heat Transf. **101**, 718-725.

[8] Bejan, A. (1982). Second-law analysis in heat transfer and thermal design, Adv. Heat Transf. **15**, 1-58.

[9] Bejan, A. (1996). Entropy generation minimization: The new thermodynamics of finite-size devices and finite-time processes, J. Appl. Phys., **79**, 1191-1218.

[10] Bejan, A. (2002). Fundamentals of exergy analysis, entropy generation minimization and the generation of flow architecture, Int. J. Energy Res. **26**, 545-565.

[11] Bejan, A. (2006). Entropy generation minimization: The new thermodynamics of finite-size devices and finite-time processes, J. Appl. Phys., **79**, 1191-1218.

[12] Cimpean, D., Lungu, N., Pop, I. (2008). A problem of entropy generation in a channel filled with a porous medium, Creative Math. & Inf., **17**, 357-362.

[13] Fersadou, I., Kahalerras, H., El, Ganaoui, M. (2015). MHD mixed convection and entropy generation of a nanofluid in a vertical porous channel, Comp. fluids, **121**, 164-179.

[14] Gbadeyan, J.A., Abubakar, J.U., Oyekunle, TL. (2020). Effects of Navier slip on a steady flow of an incompressible viscous fluid confined within spirally enhanced channel, Journal of Egyptian Mathematical Society, 28:32.

[15] Ibanez, G., Lopez, A., Pantoja, J., Moreira, J. (2016). Entropy generation analysis of a nanofluid flow in MHD porous microchannel with hydrodynamic slip and thermal radiation, Int. J. Heat Mass Transf., **100**, 89-97.

[16] Jian, Y. (2015). Transient MHD heat transfer and entropy generation in a microparallel channel combined with pressure and electroosmic effects, Int. J. Heat Mass Transf., **89**, 193-205.

[17] Khalid, A.R.A., Vatan, K. (2004). The effect of the slip condition on Stokes and couette flows due to an oscillatory wall: exact solutions., Int J NonLin Mech. **39**, 795-809.

[18] Mahmoud, M., Waheed, S. (2010). Effect of slip and heat generation absorption on MHD mixed convection flow of a micropolar fluid over a heated stretching surface, MPE, Volume, Article ID 579162.

[19] Makinde, O.D., Osalusi, E. (2006). MHD steady flow in a channel with slip at the permeable boundaries, Rom. J. Phys. **51**, 319-328.

[20] Makinde, O.D. (2012). Entropy analysis for MHD boundary layer flow and heat transfer over a flat plate with a convective surface boundary condition, Int. J. Exergy, **10**(2), 142-154.

[21] Martin, M.J., Boyd, I.D. (2016). Momentum and heat transfer in a laminar boundary layer with slip flow, JTHT. **20**(4), 710-719.

[22] Mehmood, A., Ali, A. (2007). The effect of slip condition on unsteady MHD oscillatory flow of a viscous fluid in a planar channel, Rom. J. Phys. **52**(1-2), 85-91.

[23] Nasiri, M., Rashidi, M.M., Lorenzini, G. (2015). Effects of magnetic field on entropy generation in a microchannel heat sink with offset fan shaped, Entropy, 18(1).

[24] Navier CLMH (1823). Memoire sur les lois du movement des fluids, Mem Acad R Sci Paris, **6**, 389-416.

[25] Paoletti, S., Rispoli, F., Sciubba, E. (1989). Calculation of exergetic losses in compact heat exchanger passages, ASME AES, **10**, 21-29.

[26] Shi, Z., Dong, T. (2015). Entropy generation and optimization of laminar convective heat transfer and fluid flow in a microchannel with staggered arrays of pin fin structure with tip clearance, Energy Conser. Mang., **94**, 493-504.

[27] Woods, L.C. (1975) Thermodynamics of fluid systems, Oxford, UK: Oxford University Press, J. fluid Mech., **83**, 1, 207-208.

APPENDIX

$$A = \frac{-\frac{P}{\left(M^2+\frac{1}{D_a}\right)}\left[n\alpha_1 e^{\frac{-Re}{2}}+\sinh n-\alpha_2\left(n\cosh n-\frac{Re}{2}\sinh n\right)\right]}{\left\{n(\alpha_1-\alpha_2)\cosh n+\sinh n\left[1+\alpha_1.\alpha_2\left(\frac{Re^2}{4}-n^2\right)+\frac{Re}{2}(\alpha_1+\alpha_2)\right]\right\}}$$

$$B = \frac{P}{n\alpha_1\left(M^2+\frac{1}{D_a}\right)}+\frac{A}{n}\left(\frac{1}{\alpha_1}+\frac{1}{2}\,Re\right)$$

$$A_1 = \frac{1}{8}\{(A^2\text{-}B^2)Re^2 - 4n^2(A^2-B^2) + \frac{\lambda M^2}{2}(A^2-B^2)\}$$

$$A_2 = \frac{1}{4}(Re^2+4n^2)(A^2+B^2) - 8nAB\,Re + \lambda M^2(A^2+B^2)$$

$$A_3 = \frac{1}{2}(-ARe+2nB)(-BRe+2An) + \lambda M^2 AB$$

$$A_4 = \frac{A_2}{(Re^2-RePe)}$$

$$A_5 = \frac{A_3}{(Re^2-RePe)}$$

$$A_6 = \frac{8A}{(Re^2-2RePe)}$$

$$A_7 = \frac{8B}{(Re^2-2Re\,Pe)}$$

$$A_8 = \frac{A_1}{(Re^2-Re\,Pe)}$$